

Ionic Liquid-nanoparticle Hybrid Electrolytes and Their Applications in Rechargeable Lithium Metal Batteries

Yingying Lu, Surya S. Moganty, Kevin Korf, Jennifer L. Schaefer, Shyamal K. Das, Lynden A. Archer*
*School of Chemical & Biomolecular Engineering,
Cornell University, Ithaca, New York 14853-5201

Secondary lithium metal batteries (LMBs) largely derive their improved energy storage capabilities from the high specific capacity of metallic lithium, 3860 mAh g^{-1} , which is more than ten times that of the currently used carbon anode (Figure 1).¹ However, the formation of needlelike/mushroom like electrodeposits collectively termed dendrites during electrochemical cycling leads to internal short-circuiting, premature cell failure, and potentially even more serious safety hazards.² Overcoming these effect has presented a serious obstacle in the commercialization of high energy density, rechargeable lithium metal batteries (LMBs).

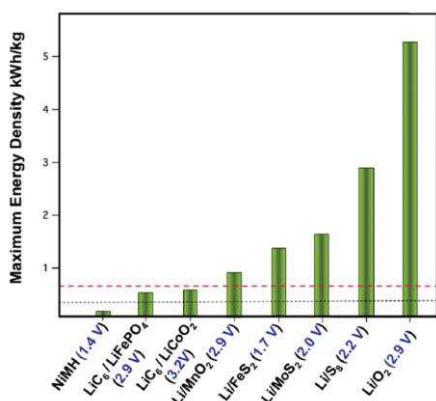
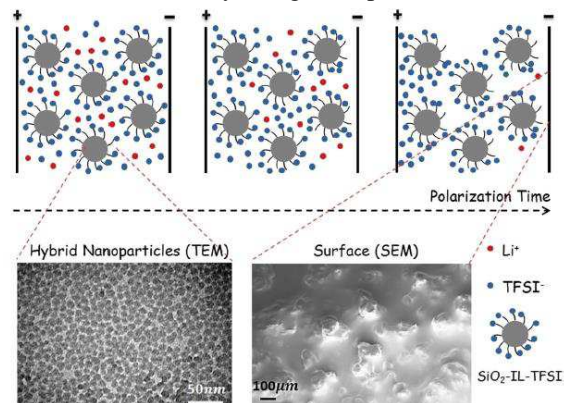


Figure 1: Theoretical specific energy and nominal voltages for various secondary/rechargeable battery electrode chemistries. The horizontal lines are the USABC medium – (black) and long-term (red) targets escalated by a factor of 3 to account for the typical factor of three increases in mass.

Many recent studies have concentrated on the electrolyte formulation, aiming at reversible stripping-plating lithium ions. Ionic liquid have for instance triggered great interest due to their low vapor pressure, non-flammability, good thermal and electrochemical stabilities. To remove the shortcomings of conventional ionic liquid such as low lithium ion transference number and low mechanical strength, we developed a family of ionic liquid-nanoparticle hybrid electrolytes ($\text{SiO}_2\text{-IL-TFSI}$, Scheme 1).^{1,3} These hybrid electrolytes are also deliberately constructed to incorporate a supporting electrolytes (extra anions and immobile cations), which theory suggests should play a decisive role in dendrite nucleation. The presence of hard nanoparticles in the electrolytes is also expected to enhance the bulk mechanical strength and to potentially improve the dielectric properties of the electrode/electrolyte interface. The former (supporting electrolyte) feature can be shown to reduce the potential gradient caused by any inhomogeneities in ion distribution during cell polarization, which reduces the electric field near the negative electrode facilitating uniform lithium deposition. The latter effect (enhanced interfacial strength) reduces the magnitude of lithium deformation during intercalation/deintercalation process because of the electrolyte's high storage modulus and may also broaden the interfacial region near the electrode/electrolyte interface over which the electrode

potential falls to zero. This feature also acts to lower the electric field near the electrode and can be shown to even cause it to fall below the threshold for dielectric breakdown of most organic electrolytes, enhancing their electrochemical stability at high cell potentials.



Scheme 1: Schematic illustration of the transient response of a $\text{SiO}_2\text{-IL-TFSI/PC}$ electrolyte during polarization of a $\text{Li}|\text{SiO}_2\text{-IL-TFSI/PC}|\text{Li}$ cell. Bottom left: TEM image of pure hybrid nanoparticles. Bottom right: SEM image of lithium metal after short-circuit by polarization.

To investigate the dendrite formation mechanism, galvanostatic polarization and cycling measurements in conjunction with a modified diffusion-convection-reaction model are employed to monitor the short-circuit phenomena caused by this uneven microstructure. To study electrochemical stability at the electrode/electrolyte interface we use a combination of linear scan voltammetry, impedance spectroscopy, and ex-situ microscopy. Finally, we demonstrate that in addition to producing orders of magnitude improvements in lithium plating efficiency and substantial enhancements in high voltage stability, the hybrid electrolytes perform well in cycling studies using Li/MoS_2 (high-energy) and Li/TiO_2 (high-power) batteries (Figure 2).

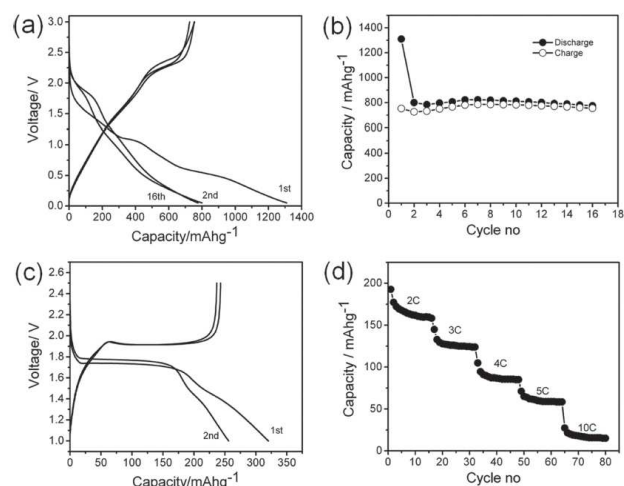


Figure 2: Galvanostatic charge-discharge curves for: (a) $\text{Li}|\text{SiO}_2\text{-IL-TFSI/PC}|\text{MoS}_2$ and (c) $\text{Li}|\text{SiO}_2\text{-IL-TFSI/PC}|\text{TiO}_2$ coin cells. Variation of capacity with cycle number for (b) $\text{Li}|\text{SiO}_2\text{-IL-TFSI/PC}|\text{MoS}_2$ and (d) $\text{Li}|\text{SiO}_2\text{-IL-TFSI/PC}|\text{TiO}_2$ cells at various current rates.

Reference

1. Y. Lu, S. K. Das and L. A. Archer *Adv. Mater.* 24, 4430-4435, 2012
2. J.M. Tarascon and M. Armand *Nature* 414, 359-367, 2001
3. Y. Lu, S. S. Moganty, J. L. Schaefer and L. A. Archer *J. Mater. Chem.* 22, 4066-4072, 2012